abstract number: **090612-059**

Numerical investigation of dynamic free-fall penetrometers in soft cohesive marine sediments using a finite element approach

Andrei Abelev, Julian Simeonov, and Philip Valent
Naval Research Laboratory,
Stennis Space Center, MS 39529,
USA

I. Introduction and scope of work

Various branches of offshore civil and petroleum engineering, as well as the Navy, have an expressed need for tools that allow for a rapid assessment of the surficial (top 2-3m) marine sediments. Undrained shear strength of soft cohesive (clayey) deposits is one of the central parameters required in these investigations. This information is critically important in evaluations of bearing capacity of sediment under the load of objects and structures placed on the sea sediment surface or embedded in it. It is also a primary parameter guiding the response of these types of sediments in resistance to dynamic penetration events, including anchors, probes, and various other bodies deployed in free fall through the water column. Dynamic free-fall penetrometers offer a potential for such rapid strength assessment and are used widely, but have typically been employed in conjunction with mostly empirical relationships to retrieve the undrained shear strength of sediments [1-5]. In this work, we analyze the behavior of a typical representative of these types of penetrometers, the STING (Sea Terminal Impact Naval Gauge). One of four available foot geometries is examined herein (50 mm), with probe configured to achieve up to 2m soil penetration. We develop an approach for modeling the velocity decay profile of the probe, as it's decelerating in the sediment after free-fall through the water column. We utilize a commercial finite-element code (ABAQUS^{TM}) to develop a full dynamic solution of the penetrometer impact and burial into marine sediment, with undrained shear strength varying linearly with depth. We conduct a comprehensive study of convergence and solution accuracy, utilizing Arbitrary Lagrangian-Eulerian dynamic remeshing schemes in a fully dynamic elasto-plastic model. We explore the conditions of fully-developed plastic flow around the foot of the penetrometer and compare our conclusions with those made utilizing other numerical approaches [6,7], primarily, due to the unavailability of laboratory controlled experimental data on the details of the plastic flow of cohesive materials around objects penetrating soft cohesive marine soils in the velocity regime of interest (O[10 m/s]). The numerical solution and prediction of the probe velocity decay, as it's penetrating the soil, is compared with the field-measured velocity time series from a STING deployment into soft marine clay.

II. Experimental evidence, existing STING algorithm, and bearing strength

STING basics

The Seabed Terminal Impact Newton Gradiometer (STING) is one of several probes that are designed to penetrate soft bottom marine sediments on impact from free-fall through the water. Key measurements include deceleration and water pressure records, allowing for correlations with depth penetrated and some description of the strength of the sediment. A schematic view of a penetrometer is shown in Fig. 1. The body of the penetrometer contains all the sensor and storage electronics and the probe is tethered via the end-cap.

Fig. 1 Schematic view of a STING penetrometer with a single extension rod and a small foot

Deployments

A large number of STING deployments in various locations of the Gulf of Mexico, Baltic, and the North Sea were performed and a comprehensive data base compiled. The seafloor sediments where the instruments were deployed were generally characterized to be soft cohesive sediments, where such methods of strength estimation of soils were appropriate.

Report Documentation Page

Form Approved
OMB No. 0704-0188

1. REPORT DATE	2. REPORT TYPE	3. DATES COVERED
JUN 2010	**N/A**	**-**

4. TITLE AND SUBTITLE	5a. CONTRACT NUMBER
Numerical investigation of dynamic free-fall penetrometers in soft cohesive marine sediments using a finite element approach	5b. GRANT NUMBER
	5c. PROGRAM ELEMENT NUMBER
6. AUTHOR(S)	5d. PROJECT NUMBER
	5e. TASK NUMBER
	5f. WORK UNIT NUMBER
7. PERFORMING ORGANIZATION NAME(S) AND ADDRESS(ES) **Naval Research Laboratory, Stennis Space Center, MS 39529, USA**	8. PERFORMING ORGANIZATION REPORT NUMBER
9. SPONSORING/MONITORING AGENCY NAME(S) AND ADDRESS(ES)	10. SPONSOR/MONITOR'S ACRONYM(S)
	11. SPONSOR/MONITOR'S REPORT NUMBER(S)

12. DISTRIBUTION/AVAILABILITY STATEMENT
Approved for public release, distribution unlimited

13. SUPPLEMENTARY NOTES
See also ADM202806. Proceedings of the Oceans 2009 MTS/IEEE Conference held in Biloxi, Mississippi on 26-29 October 2009. U.S. Government or Federal Purpose Rights License, The original document contains color images.

14. ABSTRACT

15. SUBJECT TERMS

16. SECURITY CLASSIFICATION OF:			17. LIMITATION OF ABSTRACT	18. NUMBER OF PAGES	19a. NAME OF RESPONSIBLE PERSON
a. REPORT	b. ABSTRACT	c. THIS PAGE			
unclassified	**unclassified**	**unclassified**	**SAR**	**8**	

Standard Form 298 (Rev. 8-98)
Prescribed by ANSI Std Z39-18

STING data reduction

The original STING sensor data are acquired in the form of acceleration and water pressure time series. These were processed using the standard (built-in) [1,3] algorithm, yielding a value termed "bearing strength" with depth into the sediment. STING processing involves solution of a single-point (or averaged) mass, free-falling through the water and sediment [1]:

$$ma = B + D + S - mg\,, \tag{1}$$

where m is mass, a is acceleration of the penetrometer, g is gravitational acceleration, B is buoyancy forces, D is hydrodynamic drag forces, and S resisting force of the sediment to penetration. The drag and the buoyancy forces are calculated as sums of all components acting on the penetrometer body and trailing tether line. The sediment force S is further specified as a function of "dynamic bearing strength", B:

$$B = S \,/\, \left(Ar\right), \tag{2}$$

where A – is the foot area and r is the generalized strength rate dependency factor, defined as:

$$r = \left(v \,/\, d\right)^{0.15}. \tag{3}$$

Here, v – is the velocity and d is the foot diameter. These equations allow for a determination of the bearing strength from the deceleration record of the instrument.

Contact determination

The nature of STING data reduction also involves a subjective component of determining the initial contact of the falling probe with the sediment in the recorded acceleration time-series. In stiffer sediments (of higher bearing strength) this contact point is quite obvious and, in fact, could be relegated to the automatic selection algorithm of the standard STING software. However, in soft and very soft sediments this is not the case. In such instances, which represent the bulk of the sites visited in this research, operator intervention is typically needed to correct or adjust the automatic selection interval. In such sediments, increase in penetration resistance, and consequently, change in deceleration record, is gradual enough to render the actual contact point difficult to determine. This is especially pronounced in heavier STING configurations, *i.e.* with more rod extensions and a smaller foot (*e.g.* 25mm). In these cases, operator experience in performing this procedure is the most important guiding component. Similar difficulty was encountered when estimating initial contact with soft sediments of large instrumented cylinders deployed in free-fall [8].

Noise and oscillations

In addition, for larger STING foot sizes, *e.g.* 70mm, an extraneous "noise" in deceleration time series is evident as the STING is descending through the water column. We speculate that this effect is a result of the turbulent flow regime around the larger foot (with respect to the smaller diameter shaft) that induces irregular vortex shedding, which in turn, generates oscillations in the entire probe body influencing the accelerometer signal. Averaging of the signal prior to sediment impact was used as a base-line estimate for determination of the initial point of contact. Overall, this approach yielded good and consistent results, even in very soft sediments.

Bearing strength

In the STING processing algorithm, the bearing strength, as described in Eq. 2, is used as a material parameter, rather than a concept describing sediment resistance to surface loading, as is more typical in general geotechnical applications. It is also defined as a measure of the static resistance of sediment, with all the strain-rate effects accounted by Eq. 3. This rate coefficient is constant and is preset in the software. In order to compare the bearing strength of sediment with parameters more commonly used in geotechnical practice, and subsequently apply these parameters to other solutions, a conversion first needs to occur. In general, in fine-grained and water-saturated sediments, deformation process within the sediment is occurring as an undrained process, due to the characteristic pore pressure dissipation times with respect to the time of the actual penetration event. Under these conditions, the most applicable strength parameter of cohesive (clayey) materials is the undrained shear strength. The conversion from bearing strength (static), produced by the STING processing software, to the undrained shear strength is not always trivial. Typically, similarity with the bearing capacity of footings on frictionless materials is exploited, where the bearing strength can be described as:

$$B = c_U N_c \tag{4}$$

where c_U (also often denoted as S_U) is the undrained shear strength, and N_c is the bearing capacity factor. Although this factor is a function of embedment depth for shallow burials, most algorithms use a constant value throughout the entire penetration event of between 9 and 11 for circular shapes [9-11], with the most typically chosen value being 10. This approximation of

constant N_c is especially common for probes similar to STING that penetrate to the depth of many diameters in soft sediments. In this work, we also chose the constant value of 10 for the bearing capacity factor.

Throughout most of experimental measurements conducted, STING was typically deployed with all four foot diameters, 25, 35, 50, and 70mm, at each measuring station. For most of the drops, a shaft length of 2-meters was used, except in some very soft sediments and when using the small (25mm) foot, where a shaft length of 3-meters was used to maximize penetration depth surveyed as well as to minimize chance of the body of the probe penetrating into sediment. To increase accuracy of measurements, several repeated drops (usually four) with the probe of the same configuration were performed at each drop location. Fig. 2 represents an example of the calculated undrained shear strength based on the STING algorithm for all four foot configurations, combined with the S_U (mean and standard deviation error-bars) measured using a standard laboratory vane test. Deviations of S_U measured by the various STING geometries from the vane-measured S_U are evident, suggesting that the built-in STING algorithm does not produce equally good results for all foot configurations.

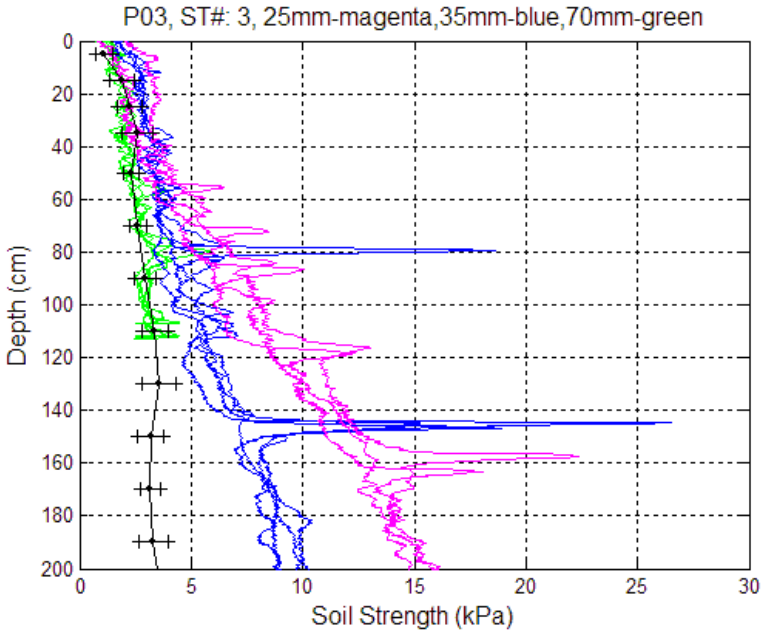

Fig. 2 Example of STING-calculated undrained shear strength, compared with that determined form lab vane tests (black curve with error-bars)

The goal of this work, therefore, is to develop an inverse finite-element-based solution utilizing full elasto-plastic formulations of STING penetration in cohesive sediments by calculating the profile of the undrained shear strength with depth from the probe deceleration record (with some assumption on the material behavior). In this paper, we discuss the initial stages of this work, where attempt is made to predict the deceleration history of the probe in one of the deployments at a location with known sediment properties. We rely on the vane shear test data for determination of the undrained shear strength, measured in the lab on undisturbed specimens recovered from the seafloor using standard gravity corers.

III. Numerical Prediction of STING Penetration

The modeling of the STING penetration problem is conducted using the commercial finite-element program ABAQUS™. The STING parameters for the reference drop were as follows: mass = 13.1 kg, foot diameter=50 mm, shaft diameter=19 mm, shaft length=2m, terminal impact velocity 4.45m/s.

Domain discretization and meshing strategy

Considering the axial symmetry of the problem, the simulations are done with two-dimensional quadrilateral axisymmetric elements which greatly reduces the computational effort. The dimensions of the model domain (Fig. 3a), 3m in the vertical and 1m in the horizontal, were chosen to accommodate the observed penetration depth of the STING in the reference drop and to place the artificial outer and bottom boundaries sufficiently far from the penetrating body to avoid any numerical influence on the overall solution. The fully dynamic solutions involving large soil deformation are obtained using the Arbitrary Lagrangian-Eulerian (ALE) remeshing capabilities of an ABAQUS/Explicit analysis.

Even with very frequent ALE remeshing, a special initial mesh is needed to alleviate the extreme compression of the soil element just below the STING foot (Fig. 3b). Furthermore, the resolution under the foot decreases with time as the STING penetrates deeper because some of the nodes contacting the foot slide past the corner during the plastic flow. To ensure sufficient resolution near the corner of the foot, it was therefore necessary to increase the mesh density toward the axis of symmetry. These requirements result in a mesh where the initial elements under the STING foot have very large (~40) vertical to horizontal aspect ratio. The initial mesh was created using 150 uniformly distributed elements in the vertical and 200 elements in the horizontal with a non-uniform spacing such that the horizontal step near the axis is 50 times smaller than that near the outer domain. It was necessary to apply the ALE remeshing for the considered reference simulation at every time increment with two mesh sweeps per increment. The ALE mesh control objective was set at preserving the initial mesh grading rather than improvement (reduction) of the aspect ratio.

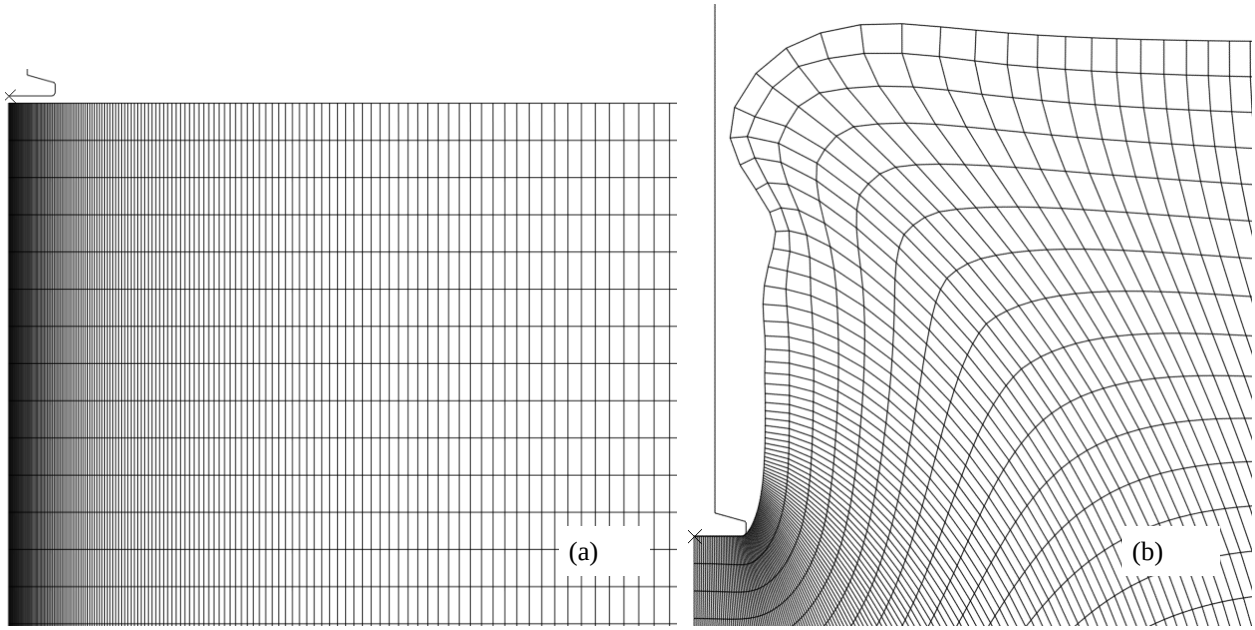

Fig. 3. (a) Model geometry and initial mesh near the STING contact area, (b) typical mesh distortion in a fully dynamic penetration simulation

Constitutive models

The soil was modeled as an elastic-perfectly-plastic continuum material with density, ρ, of 1600 kg/m^3, Young's modulus, E, of 10 MPa, Poisson ratio, ν, of 0.45, and the von Mises plastic yield criterion with depth dependent shear strength c_U. For simplicity, we assume that shear strength increases linearly with depth:

$$c_U(z) = c_U(0) + \alpha z \tag{5}$$

where α is a constant. A linear fit to the vane and fall-cone test data (Fig. 4) was selected with the soil surface intercept of 1.0 kPa the line slope of 4.0 kPa/m. The mechanical interaction between the STING surface and the soil is modeled using the penalty friction formulation for tangential behavior with maximum shear stress τ_{max} equal to that of $c_U(0)$ = 1.0 kPa. We use a large friction coefficient of 100 to simulate the material behavior as closely as possible to the rigid-perfectly-plastic as possible. For the normal behavior we use the default hard contact formulation where the normal stress is fully transmitted between contacting surfaces.

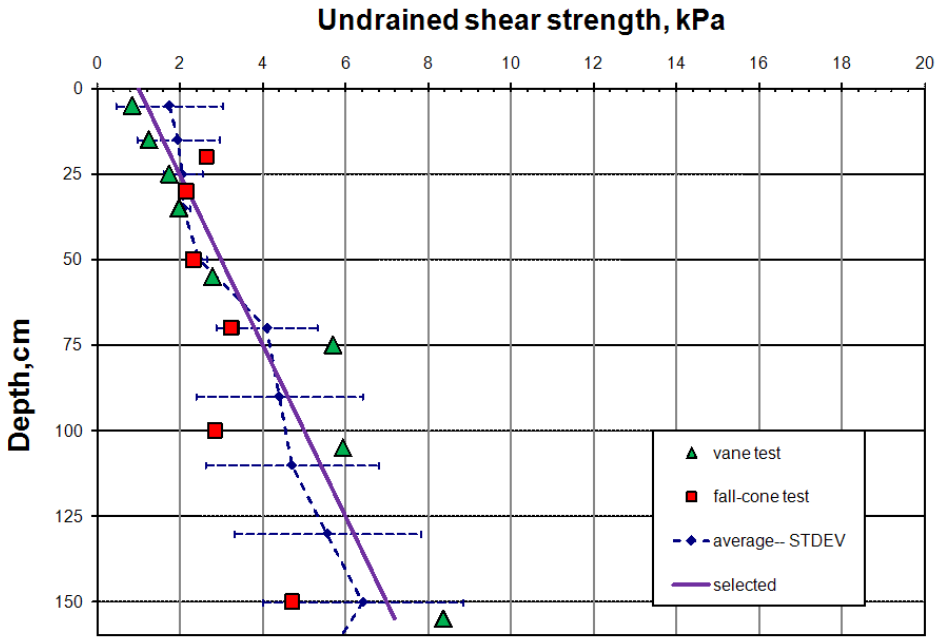

Fig. 4. Undrained shear strength variation with depth, measured in vane test, fall-cone test, average values, standard deviation (error-bars), and the selected linear profile

Analysis steps, loading and boundary conditions

The boundary conditions for the penetration simulations consist of assuming zero normal displacement on the bottom and the outer (right) boundaries. No boundary conditions are imposed on the top boundary so that the soil can be freely displaced upwards by the intruding STING. In preliminary calculations, we found that including the geostatic pressure due to the soil own weight was essential for realistic damping of the STING momentum. Subjecting the initially unloaded soil mass to gravity results in undesirable elastic waves, which must be damped in order to reach the static equilibrium of soil pressure and gravity. In the software used, ABAQUS, this pre-stressing in fully dynamic formulations remains an acknowledged difficulty. This self-weight loading equilibration process is simulated in a separate step, preceding the main penetration analysis step. To further expedite the loading oscillations decay process in this gravity step, the following procedure is adopted. The gravity amplitude g is gradually increased from zero to its nominal value g = 9.8 m/s^2 over a short period of 0.1 s and is then kept constant for the remaining 0.4 s of this time step. The elastic waves were damped over this period to a negligible amplitude by applying a (damping) viscous pressure load on the top surface, proportional to the surface normal velocity (only for this part of the solution step).

This gravity step was followed by the main penetration step where the STING was released with initial velocity, as measured in the test by the probe, of 4.45m/s at the soil surface. We further assume that just before impacting the bottom, the buoyancy, gravity and water drag terms in equation (1) are in balance, *i.e.* the probe has reached terminal condition. This leads to the assumption that the STING deceleration is entirely due to soil resistance and soil inertial effects. Accordingly, gravity, water drag, and buoyancy are not applied on the STING during the main step.

Results

The penetration dynamics are illustrated here by the instantaneous distributions of the Mises stress (Fig. 5) and the equivalent plastic strain (Fig. 6) at three different depths during the STING penetration. Fig. 5c shows that the Mises stress reaches maximum amplitude of 3600 Pa and that the region maximum stress can reach as far as 10 foot diameters (50cm) away from the probe's foot. The stresses on the bottom and the outer boundaries however are relatively small. Thus, the domain seems to be large enough so that the impact of the artificial boundaries on the penetration dynamics is negligible. The region of plastic failure (Fig. 6) is much narrower and extends only about 1-2 foot diameters in the radial direction and about half a diameter beneath the tip of the STING. The plastic equivalent strain in Fig. 6 is defined as the time integral of:

$$\dot{\bar{\varepsilon}}^{pl} = \sqrt{\tfrac{2}{3}\dot{\varepsilon}^{pl} : \dot{\varepsilon}^{pl}} \,. \qquad (6)$$

The present results for the extent of the plastic zone agree with those in reference [7], where similar ABAQUS simulations are done for cone penetration. Reference [6], on the other hand, estimates, using a quasi-steady analysis, that the plastic zone for a cone penetration can reach up to 10 cylinder diameters. This is not necessarily inconsistent as the simulations in [6] consider less rigid soils with smaller Young's modulus (E). In view of the dependence of the plastic zone on E , it will be important to

extend the present result with a parametric investigation of the effect of E. It is also worth noting that the maximum stress (Fig. 5c) is located outside the plastic zone (Fig. 6c). In Fig. 7, the predicted STING velocity (dashed line) is compared directly with the measured velocity (solid line). The agreement is good in the first 50 cm of penetration but the two curves diverge below this depth somewhat, and the velocity discrepancy reaches 0.5 m/s by the time the STING foot reaches 1.5 m depth. On the other hand, there is a better agreement at larger depths with respect to the rate at which velocity changes with depth, i.e. the slope of the curves (acceleration).

The somewhat larger slope discrepancies at shallower depths might result from neglecting the effect of rate-dependent hardening. This effect may be more pronounced earlier in the penetration when the STING is moving with larger velocity and the soil experiences larger deformation rates. The reference STING drop considered here will be used for additional analysis where the constitutive model is augmented with a Johnson-Cook-type hardening law for the yield stress, reflecting the power-dependency of sediment shear strength on the rate of loading ([12]).

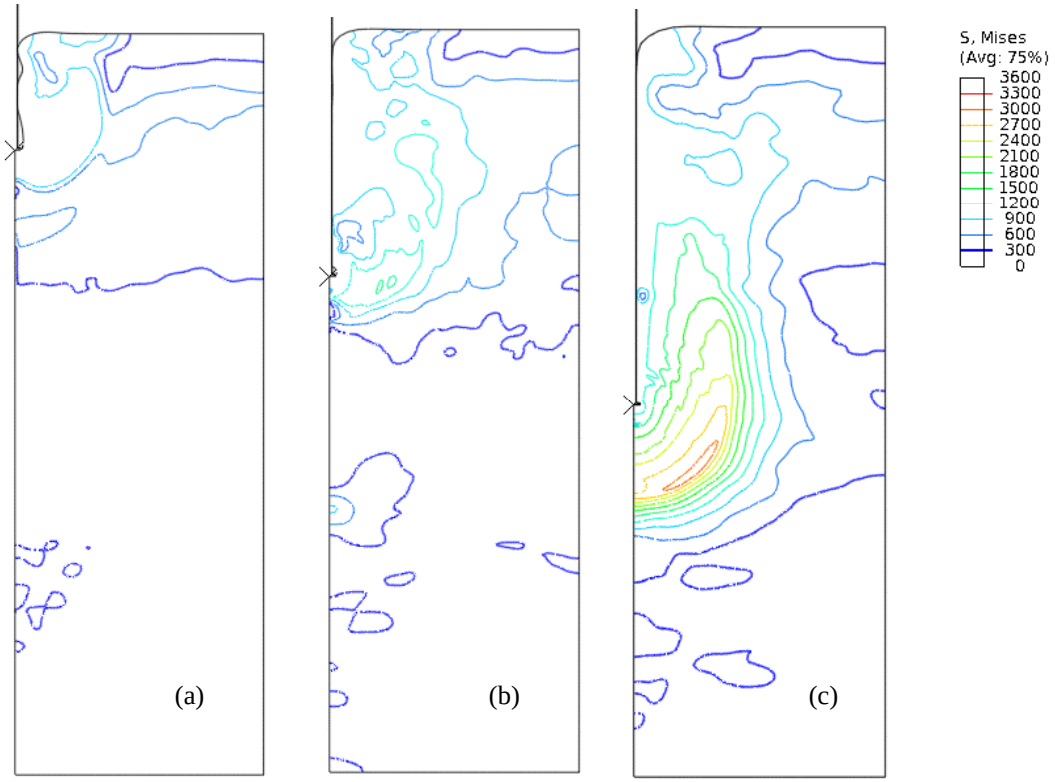

Fig. 5. Mises stress at different times corresponding to STING foot depths z = 47cm (a), 100cm (b) and 152cm (c). Domain size: 1x3 m

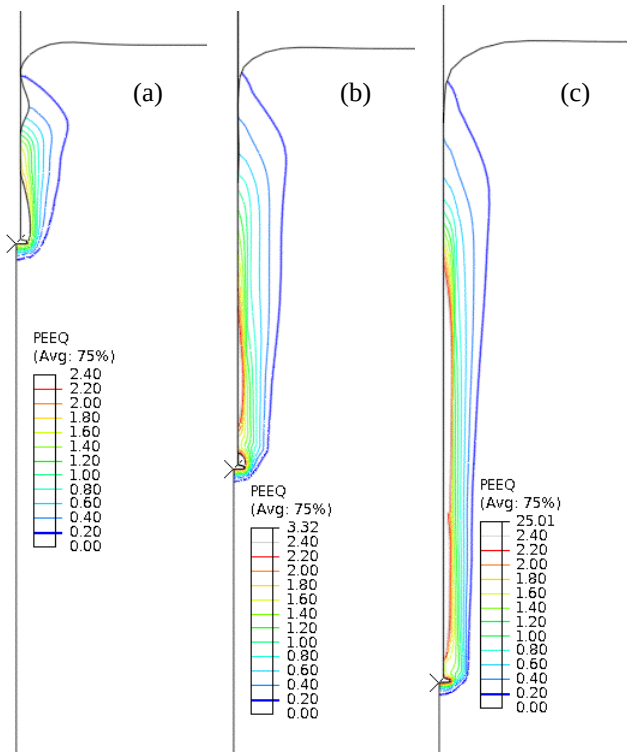

Fig. 6. Contours of plastic equivalent strain at times corresponding to STING foot depths z = 47cm (a), 100cm (b) and 152cm (c). Only part of the entire domain is shown

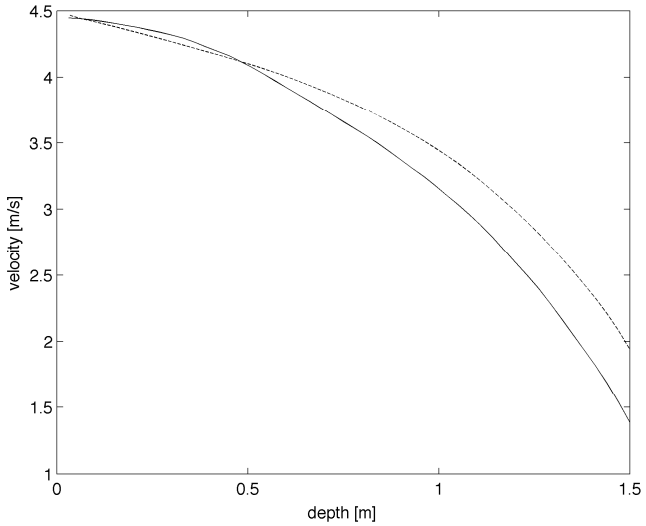

Fig. 7. Modeled (dash) and observed (solid) STING velocity as a function of depth

IV. SUMMARY AND DISCUSSION

This paper represents the first stage in developing an algorithm for extracting the values of the undrained shear strength from the deceleration records of the STING penetrometer. A brief summary of the STING penetrometer and its processing algorithm is given. Then, we focus on the direct simulations of the probe velocity decay with depth, using simple soil constitutive models in a fully-dynamic elasto-plastic analysis. Much attention is devoted to alleviating severe numerical problems when analyzing a problem with extreme deformation, leading to mesh distortions and thus necessitating efficient remeshing methods. Arbitrary Lagrangian-Eulerian, ALE, remeshing mechanics of ABAQUS[5] software is effectively utilized, allowing the solution to proceed and yielding good agreement with the velocity profile recorded by the decelerating STING penetrometer in situ. The soil is modeled as von Mises material with yield strength derived from a combination of laboratory vane and fall-cone tests and assuming a strength profile linear with depth. The methodology developed allows for the large-deformation penetration to

proceed, and yields good agreement with the in-situ data. The future work will focus on the ultimate goal of the project, *i.e.* of developing an algorithm for extracting the strength profile from the field-measured deceleration record via inverse solutions in ABAQUS.

V. Acknowledgments

This research is supported by Program Element No. 61153N of the Naval Research Laboratory and the Office of Naval Research. The help of the crews and research teams, much too numerous to list here but instrumental in obtaining the field data including penetrometer records is greatly appreciated. This work was also supported in part by a grant of computer time from the DoD High Performance Computing Modernization Program at the NAVY DSRC and the ERDC DSRC.

VI. References

[1] R. Poeckert, J. Preston, T. Miller, R. Religa, and A. Eastgaard, *A seabed penetrometer. DREATechnical Memorandum*, Dartmouth, Nova Scotia: 1997.

[2] R.D. Stoll and T. Akal, "XBP- Tool for Rapid Assessment of Seabed Sediment Properties," *Sea Technology*, vol. 40, 1999, pp. 47-52.

[3] Jasco Research Ltd., *STING Mk.II - Underwater Sediment Bearing Strength Probe. User's Manual*, R-Hut, University of Victoria Campus Victoria, British Columbia: 2002.

[4] R.M. Beard, "Expendable Doppler Penetrometer for Deep Ocean Sediment Strength Measurements.," 1984.

[5] R. Beard, N.C.B. Center, and C.A. Port Hueneme, "A Penetrometer for Deep Ocean Seafloor Exploration," *OCEANS*, 1981.

[6] Q. Lu, M. Randolph, Y. Hu, and I. Bugarski, "A numerical study of cone penetration in clay," *Geotechnique*, vol. 54, May. 2004, pp. 257-267.

[7] M.Z. Tekeste, R.L. Raper, E.W. Tollner, and T.R. Way, "Finite element analysis of cone penetration in soil for prediction of hardpan location," *TRANSACTIONS OF THE ASABE*, vol. 50, Feb. 2007, pp. 23-31.

[8] A.V. Abelev, P.J. Valent, and K.T. Holland, "Behavior of a large cylinder in free-fall through water," *IEEE Journal of Oceanic Engineering*, vol. 32, Jan. 2007, pp. 10-20.

[9] L. Satkowiak, *Modified NCSC impact burial prediction model with comparisons to mine drop tests*, Panama City, FL: Naval coastal systems center, 1991.

[10] R. Hurst and S. Murdoch, "Measurement of sediment shear strength for mine impact burial predictions," Auckland, New Zealand: DSTO, 1991, p. 8.

[11] A. Skempton, "The bearing capacity of clays," *Proc. Bldg. Research Congress*, 1951.

[12] A. Abelev and P.J. Valent, "Strain-rate dependency of strength and viscosity of soft marine deposits of the Gulf of Mexico," Biloxi, MS: 2009.